

Effective nonlinear optical properties in compositionally graded films: Analytical and numerical calculations

B. Liu,^{1,2} L. Gao,^{1,*} and K. W. Yu³

¹*Department of Physics, Suzhou University, Suzhou 215006, China*

²*Department of Physics, Jiangsu Teachers, University of Technology, Changzhou 213001, China*

³*Department of Physics, The Chinese University of Hong Kong, Shatin, NT, Hong Kong, China*

(Received 7 July 2005; revised manuscript received 13 October 2005; published 28 December 2005)

Effective nonlinear optical properties of compositionally graded films, in which the volume fraction of nonlinear metal particles varies along the direction perpendicular to the films, are theoretically and numerically investigated. Theoretically, we first adopt effective medium approximation to derive equivalent linear dielectric constant and third-order nonlinear susceptibility in a z -slice. Then, the formulas for effective nonlinear optical properties of the graded film are established, if we regard the graded film as a multilayer one. Numerically, random resistor-capacitor networks are used to simulate our system. We find that the surface plasmon resonant bands and the optical nonlinearity enhancement magnitude for compositional graded profile become broader and larger than those in the nongraded case. Moreover, for a graded profile $p(z)=az^m$, increasing a (or decreasing m) is helpful to broaden the resonant bands. To one's interest, there exist two enhancement peaks in the frequency region $0.4\omega_p \leq \omega \leq 0.6\omega_p$, which are not predicted by our approximate theory. Otherwise, our theoretical results are found to be in good agreement with numerical simulation data.

DOI: [10.1103/PhysRevB.72.214208](https://doi.org/10.1103/PhysRevB.72.214208)

PACS number(s): 42.65.-k, 72.20.Ht, 77.84.Lf

I. INTRODUCTION

Nonlinear optical properties of metal-dielectric composites have received much attention over the years because of their potential applications in engineering and technology.¹⁻³ For instance, the large optical nonlinearity and figure of merit in these materials are of importance in industrial applications such as ultrafast switching, signal regeneration and high speed demultiplexing.⁴

Recently, graded materials have attracted considerable interest in various engineering applications due to their different physical properties from the homogenous materials and conventional composite ones.⁵ In nature, there exist many graded materials, such as biological cells⁶ and liquid crystal droplets.⁷ In experiments, a graded structure may be produced by using various approaches such as deformation under large sliding loads⁸ and adsorbate-substrate atomic exchange during growth.⁹ As graded materials are the materials whose physical properties can vary continuously in space, the traditional theories fail to deal with the composites of graded material. In order to investigate the effective nonlinear optical properties of graded composites, we have established a first-principles approach and a nonlinear differential effective dipole approximation (NDEDA).¹⁰ To one's interest, it was found that the presence of the physical gradations is helpful to realize appreciable optical nonlinearity.¹⁰ Alternatively, the graded metallic films were also found to possess large nonlinear optical properties.^{11,12}

In addition to the graded composites mentioned above, spatially graded composites are a new generation of functional materials in which the geometric parameters such as the composition or microstructure morphology (rather than the local physical parameters) are gradually varied in one or more dimensions.¹³ These materials have been successfully manufactured for various applications.^{14,15} For instance, in

metal-ceramic graded composites, a continuous trade-off of fracture toughness and high thermal conductivity of metals is made with ceramic hardness and low thermal conductivity. In addition, in heat and impact protection applications, the material multifunctionality consists of the ability to provide structural support by virtue of the metallic portions of graded materials.¹⁵ Based on effective medium approximation and numerical simulation, Hui *et al.* investigated effective thermal conductivity of the graded thin film with compositional gradient.¹⁶ More recently, optical nonlinearity enhancement in compositionally graded metal/dielectric film was calculated.¹⁷ In this paper, we would like to investigate the effective linear and nonlinear optical properties in spatially graded metal/dielectric films both theoretically and numerically. To account for the equivalent linear dielectric constant and nonlinear optical susceptibility, we resort to Bruggeman effective medium approximation¹⁸ in conjunction with spectral representation theory.¹⁹ As consequence, our formulas can be valid for all volume fractions of nonlinear metal particles. Moreover, the approximate theory takes into account the physical anisotropy in such a compositionally graded film. To verify the validity of our theory, we then take one step forward to perform numerical simulations on random nonlinear resistor-capacitor networks, which has been widely applied with the success to study nonlinear optical properties in random composites.²⁰⁻²⁴ To the best of our knowledge, there is no existing simulation data on nonlinear optical properties in the compositionally graded films. We shall show that the theory provides good descriptions of numerical simulation data on linear optical absorption spectra and describes simulation data on optical nonlinearity reasonably. Especially, numerical simulation data show that there exist two dominant peaks in the middle frequency region, which can not be described by our theory.

We turn now to the body of the paper. We describe the model and present our theory in Sec. II. A description of the

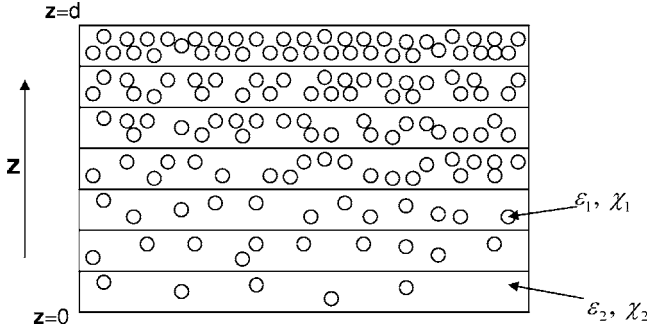


FIG. 1. The functionally graded films with width d along z axis.

model of numerical simulations is given in Sec. III. In Sec. IV, numerical simulation data and theoretical results are shown. The paper ends with a discussion and conclusion in Sec. V.

II. MODEL AND THEORY

We consider nonlinear metal/dielectric compositionally graded films with width d along the z axis (see Fig. 1). For a slab of material at position z , a volume fraction $p(z)$ of metallic materials with linear dielectric constant ϵ_1 and third-order nonlinear optical susceptibility χ_1 , and dielectrics with ϵ_2 and χ_2 are distributed at random. We restrict our discussion in a weakly nonlinear case, i.e., the nonlinear term of the component $\chi_i |\mathbf{E}|^2$ ($i=1,2$) is assumed to be weak in comparison with the linear one ϵ_i . To realize compositional graded films, $p(z)$ is chosen to vary only in the z direction. Without loss of generality, we take the bottom and the top of the films to lie at $z=0$ and $z=d$.

Generally, it is impossible to calculate equivalent (local) dielectric constant $\bar{\epsilon}(z)$ and nonlinear susceptibility $\bar{\chi}(z)$ exactly in terms of $p(z)$ for a z -slice. Here, we resort to three-dimensional effective medium approximation (EMA) for estimating these local physical properties. For $\bar{\epsilon}(z)$, EMA reads,¹⁸

$$p(z) \frac{\epsilon_1 - \bar{\epsilon}(z)}{\epsilon_1 + 2\bar{\epsilon}(z)} + [1 - p(z)] \frac{\epsilon_2 - \bar{\epsilon}(z)}{\epsilon_2 + 2\bar{\epsilon}(z)} = 0. \quad (1)$$

To first order in χ_i , the local (equivalent) nonlinear susceptibility $\bar{\chi}(z)$ is given by^{25,26}

$$\begin{aligned} \bar{\chi}(z) |\mathbf{E}_0|^2 \mathbf{E}_0^2 &= p(z) \chi_1 \langle |\mathbf{E}_{\text{lin},1}|^2 \mathbf{E}_{\text{lin},1}^2 \rangle \\ &+ [1 - p(z)] \chi_2 \langle |\mathbf{E}_{\text{lin},2}|^2 \mathbf{E}_{\text{lin},2}^2 \rangle \\ &\approx p(z) \chi_1 \langle |\mathbf{E}_{\text{lin},1}|^2 \rangle \\ &\times \langle \mathbf{E}_{\text{lin},1}^2 \rangle + [1 - p(z)] \chi_2 \langle |\mathbf{E}_{\text{lin},2}|^2 \rangle \langle \mathbf{E}_{\text{lin},2}^2 \rangle, \end{aligned} \quad (2)$$

where $\mathbf{E}_{\text{lin},i}$ means that the linear local field is to be taken from the solution to the linear problem when the external field \mathbf{E}_0 is applied at position z , while $\langle \dots \rangle$ means the spatial average. Note that the decoupling treatment has been adopted in Eq. (2).^{27,28}

Within the spectral representation theory, the averages of spatial local fields are expressed as¹⁹

$$\langle \mathbf{E}_{\text{lin},1}^2 \rangle = \frac{1}{p(z)} \int_0^1 \left(\frac{s}{s-x} \right)^2 m(x) dx \mathbf{E}_0^2,$$

$$\langle \mathbf{E}_{\text{lin},2}^2 \rangle = \frac{1}{1-p(z)} \left[1 - \int_0^1 \frac{s^2-x}{(s-x)^2} m(x) dx \right] \mathbf{E}_0^2, \quad (3)$$

and

$$\langle |\mathbf{E}_{\text{lin},1}^2| \rangle = \frac{1}{p(z)} \int_0^1 \left| \frac{s}{s-x} \right|^2 m(x) dx |\mathbf{E}_0|^2,$$

$$\langle |\mathbf{E}_{\text{lin},2}^2| \rangle = \frac{1}{1-p(z)} \left[1 - \int_0^1 \frac{|s|^2-x}{|s-x|^2} m(x) dx \right] |\mathbf{E}_0|^2, \quad (4)$$

where $s \equiv \epsilon_2 / (\epsilon_2 - \epsilon_1)$, and the spectral density function $m(x)$ for three-dimensional system is given by

$$\begin{aligned} m(x) &= \frac{3p(z)-1}{2} \theta[3p(z)-1] \delta(x) \\ &+ \begin{cases} \frac{3\sqrt{(x-x_1)(x_2-x)}}{4\pi x} & \text{if } x_1 < x < x_2 \\ 0 & \text{otherwise,} \end{cases} \end{aligned}$$

where $\theta(\dots)$ is the step function and $x_{1,2} = \{1 + p(z) \mp 2\sqrt{2p(z)[1-p(z)]}\}/3$.

In what follows, we aim at studying the effective linear dielectric constant ϵ_e and effective third-order nonlinear susceptibility χ_e of the composite films. Actually, since $\bar{\epsilon}(z)$ and $\bar{\chi}(z)$ are known for each z -slice, the problem reduces to the one of multilayers.²⁹ If the electric field is polarized perpendicular to the planes of the graded films, the effective linear dielectric constant ϵ_{eff}^z is given by

$$\frac{1}{\epsilon_{\text{eff}}^z} = \frac{1}{d} \int_0^d \frac{dz}{\bar{\epsilon}(z)}, \quad (5)$$

and the effective third-order nonlinear susceptibility χ_{eff}^z is given by

$$\chi_{\text{eff}}^z = \frac{1}{d} \int_0^d \bar{\chi}(z) \left| \frac{\epsilon_{\text{eff}}^z}{\bar{\epsilon}(z)} \right|^2 \left(\frac{\epsilon_{\text{eff}}^z}{\bar{\epsilon}(z)} \right)^2 dz. \quad (6)$$

For electric field polarized in the plane of layers, ϵ_{eff}^x and χ_{eff}^x are given by a simple integral, i.e.,

$$\epsilon_{\text{eff}}^x = \frac{1}{d} \int_0^d \bar{\epsilon}(z, \omega) dz, \quad (7)$$

and

$$\chi_{\text{eff}}^x = \frac{1}{d} \int_0^d \bar{\chi}(z, \omega) dz. \quad (8)$$

III. NUMERICAL SIMULATION

To test the validity of our theory, one represents the graded film as a random nonlinear resistor-capacitor net-

work. The network is assumed to be a simple cubic lattice consisting of $L_x \times L_y \times L_z$ sites, where L_j is the number of layers along j axis ($j=x, y, z$). To modify the compositional gradient, in a z -slice, the bonds are occupied by the nonlinear metal component with probability $p(z)$, and occupied by the nonlinear dielectric component with probability $1-p(z)$. (The z coordinate of bonds parallel to z axis is taken as that of the midpoint). The current i -voltage v responses of two components has the form

$$i = g_k v + \chi_k |v|^2 v \quad (k=1,2), \quad (9)$$

where g_k is the linear admittance and χ_k is termed as third-order nonlinear susceptibility. Again, weak nonlinearity indicates that $\chi_k |v|^2 \ll g_k$. To model the mixtures of metallic and insulating components at finite frequencies, we take g_1 and g_2 to be

$$g_1 = \frac{1 + i\omega RC - \omega^2 LC}{R + i\omega L} \quad (10)$$

and

$$g_2 = i\omega C', \quad (11)$$

where R is the resistance of conducting element, L is its inductance, C is a capacitance, and C' is the capacitance of insulating element. If we let $C=C'$, and introduce the plasma $\omega_p=(LC)^{-1/2}$ and the relaxation time $\tau=L/R$, then the ratio g_1/g_2 takes Drude-like form,

$$\frac{g_1}{g_2} = 1 - \frac{\omega_p^2}{\omega(\omega + i/\tau)} \quad (12)$$

For numerical simulations, we choose units such that $L=C=C'=1$. This choice has been widely made in studying the frequency response in random composites.^{23,24} As a result, we have units $\omega_p=1$ and $\tau=10$. As far as the nonlinear susceptibilities are concerned, we assume χ_1 to be independent of frequency, and for simplicity, χ_2 is set to be zero.

The aim here is to simulate the effective linear admittance and nonlinear susceptibility of the networks, which are defined in the following way. For a given graded profile, we have the equivalent responses of a full uniform network of identical nonlinear conductors, each of which has a response of the form

$$i = g_{eff} v_0 + \chi_{eff} |v_0|^2 v_0, \quad (13)$$

where g_{eff} and χ_{eff} , respectively, are the effective linear admittance and nonlinear susceptibility of the network. and $v_0 \equiv V_0/L_z$ (or V_0/L_x).

Since the graded film possesses anisotropic physical properties, we first assume that the planes $z=0$ and $z=L_z$ are held at potentials 0 and V_0 . In this connection, we have $\mathbf{E}=E\mathbf{e}_z$, corresponding to a p -polarized wave. On the other hand, free boundary conditions (By "free" we mean that the nodes at $x=0$ and $x=L_x$ are connected only to other bonds at the same x value, and to internal nodes) are imposed in the x direction, while periodic boundary conditions are imposed in the y direction to illustrate that every slice is a boundless film along

the y axis. When the field is applied along the z axis, we can numerically simulate the effective linear and nonlinear responses, denoted by g_{eff}^z and χ_{eff}^z .

Our simulations are carried out for the system on $10 \times 10 \times 30$ cubic lattices. (L_z is large because each value of the metal filling fraction is varied in z direction. We also carry on $10 \times 10 \times 40$ cubic lattices, and find that the results change little). The size of the simulation network is sufficient as we are not focusing on the percolation problem. During simulation, 50 different configurations are averaged over. For each configuration, we apply Kirchhoff's law to each of the nodes relating the potential of the node (v_ν) to those of its six neighbors (v_μ),

$$\sum_{\mu=1}^6 g_\mu (v_\mu - v_\nu) = 0, \quad (14)$$

where g_μ is the linear admittance of the bond μ . In numerical simulation, we first solve the potentials at all nodes with Eq. (14), and g_{eff}^z can be directly extracted by²⁰⁻²²

$$g_{eff}^z = \frac{1}{v_0} \sum_{\alpha} g_{\alpha} \delta v_{\alpha}, \quad (15)$$

where the summation is over all bonds and δv_{α} is the potential difference (voltage) across the bond α . Note that the relation between g_{eff}^z and ϵ_{eff}^z is $g_{eff}^z = i\omega \epsilon_{eff}^z$.

The effective nonlinear susceptibility is given by^{21,22,30}

$$\chi_{eff}^z = \frac{\sum_{\alpha} \chi_{\alpha} |\delta v_{\alpha}|^2 \delta v_{\alpha}^2}{v_0^4}, \quad (16)$$

Eq. (16) is the discrete analog of Eq. (2), which suggests that the effective nonlinear susceptibility can be obtained by finding the voltages at the nodes of the random network in the absence of χ_1 , i.e., in the corresponding linear random network problem with the nonlinear term χ_i turned off. Therefore, the resultant voltages from Eq. (14) are used to calculate the effective nonlinear coefficient [see Eq. (16)].

Similarly, the linear admittance g_{eff}^x and nonlinear susceptibility χ_{eff}^x in the x direction are also simulated. In this case, the volume fraction is still gradually varied in the z direction. However, the planes $x=0$ and $x=L_x$ are held at potentials 0 and V_0 , free and periodic boundary conditions are imposed in the z direction and y direction, respectively.

IV. NUMERICAL RESULTS

In what follows, we present numerical results based on numerical simulations and our theory. For simplicity, we let $d=L_z$. First, we investigate the effective linear and nonlinear responses of the compositionally graded films with graded profile $p(z)=z/d$. The case for nongraded profile $p(z)=1/2$ is also plotted for comparison, as both profiles yield the same amount of metal component, i.e.,

$$\frac{1}{d} \int_0^d dz \frac{z}{d} = \frac{1}{d} \int_0^d dz \frac{1}{2} = \frac{1}{2}. \quad (17)$$

In Fig. 2, we show the real part of effective linear response $\text{Re}(g_{eff}^z)$ versus the normalized frequency ω/ω_p for the case

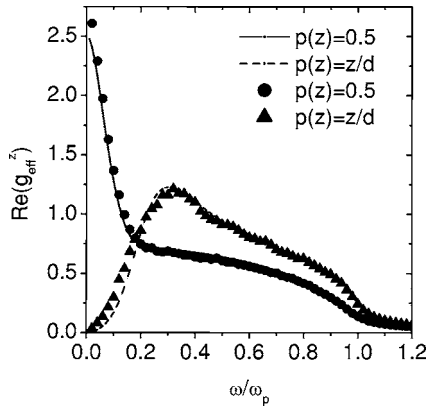


FIG. 2. Real part of effective linear response $\text{Re}(g_{\text{eff}}^z)$ for p -polarized light as a function of the normalized frequency ω/ω_p for compositional graded profile $p(z)=z/d$ and nongraded profile $p(z)=1/2$. The curves are theoretical results, and the symbols represent numerical simulation data.

that the electric field is polarized along z axis. In random composites with nongraded profile $p(z)=1/2$, the metal component is larger than its percolation threshold $p_c=1/3$, and it can easily form an infinite cluster through the whole composite. As a result, there exists a Drude peak in the vicinity of zero frequency, in addition to a surface plasmon resonant band.²³ However, when the graded profile $p(z)=z/d$ is taken into account, the surface resonant band becomes more visible than the one in the case of nongraded films, and the Drude peak around zero frequency vanishes. The disappearance of the peak can be understood as follows. For graded profile $p(z)=z/d$, as the volume fraction of metal component at

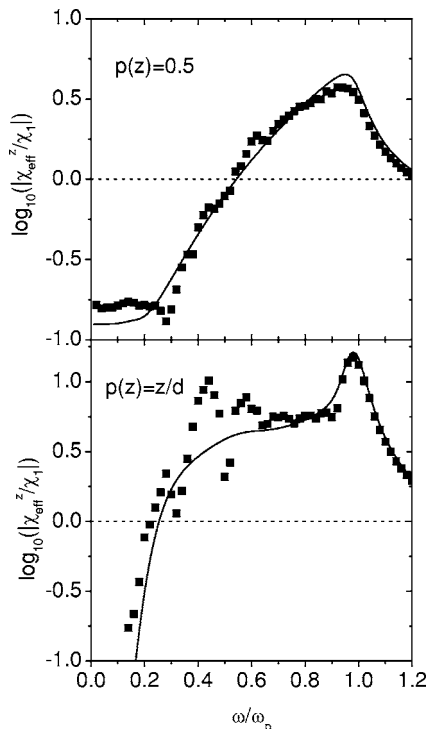


FIG. 3. Same as Fig. 2, but for effective optical nonlinearity enhancement $|\chi_{\text{eff}}^z/\chi_1|$ for p -polarized light as a function of ω/ω_p .

small z slice will be smaller than $1/3$, these slices will be not metallic. In an analogy with capacitors in series, the whole graded film will always be insulating, and hence no Drude peak appears when the electric field is polarized along the z axis. Moreover, the good agreement between our theory and simulation results is obviously found.

In Fig. 3, we study the modulus of the effective third-order optical nonlinearity enhancement $|\chi_{\text{eff}}^z/\chi_1|$ as a function of the normalized frequency ω/ω_p . We find that the optical nonlinearity enhancement for graded and nongraded profiles is quite different, although the total volume fractions of the systems are the same. In detail, for compositional gradation, the enhancement band becomes broader and the enhancement magnitude is larger than those for the nongraded case. The differences mainly result from the fact that for the graded structure, there are much more isolated metallic clusters in small z -slices, which is helpful to enhance the surface plasmon effect and thereby the maximum of the optical nonlinearity. Therefore, for a given total volume fraction, we can choose a suitable compositional gradation profile to achieve appreciable enhancement of optical nonlinearity. According to simulation results, we predict that there exist two resonant peaks in addition to one around the plasma frequency ω_p . The latter peak can be well described by effective medium approximation, which predicts a strong dispersive ϵ_e with a small imaginary part just beyond the band edge, resulting in a sharp peak. The former resonant peaks may be expected because the network model is quite different from continuum model, and they reflect the occurrence of isolated clusters of a few bonds (lattice animals) at the lower volume fraction

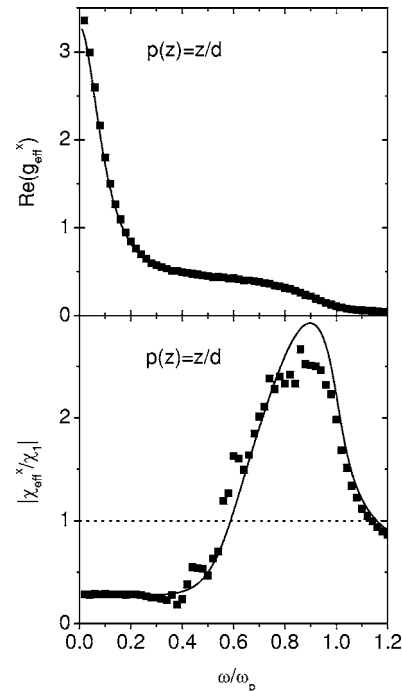


FIG. 4. Real part of effective linear response $\text{Re}(g_{\text{eff}}^x)$ and effective optical nonlinearity enhancement $|\chi_{\text{eff}}^x/\chi_1|$ for s -polarized light as a function of the normalized frequency ω/ω_p for compositional graded profile $p(z)=z/d$. The curves are theoretical results, and the symbols represent numerical simulation data.

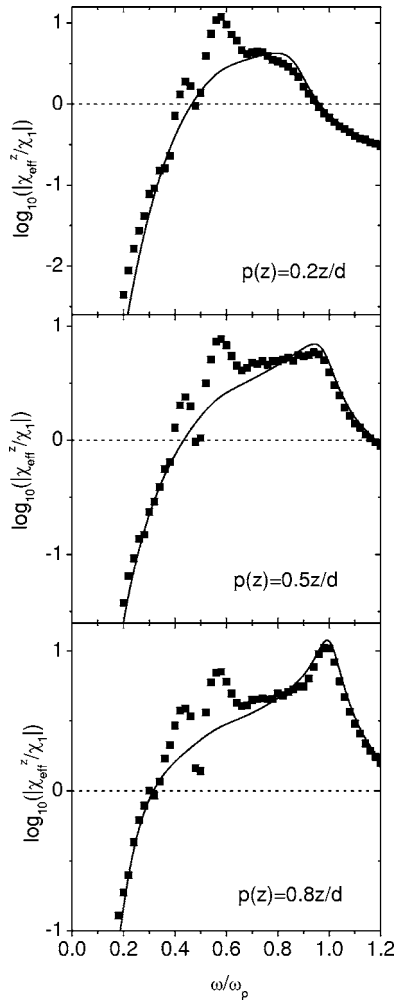


FIG. 5. Same as Fig. 2, but for power-law grade profile $p(z) = az^m$ with $m=1$ and different a .

region of the networks.^{21,22} Furthermore, the discrepancies between simulation data and our theory are quite reasonable in that our theory, being a mean-field approximation neglects the local field fluctuation (such an effect becomes much stronger for the gradient profile), to which $|\chi_{eff}^z/\chi_1|$ is very sensitive.

Next, we have similar considerations for the electric field polarized parallel to the plane of layers, as shown in Fig. 4. It is observed that the results for $p(z)=z/d$ are quite similar to those in random composites with $p(z)=1/2$. Actually, in this case, the effective linear admittance can be obtained as the problem of the conductors in parallel. Therefore, the metallic character at large z -slice results in the metallic behavior of compositionally graded film. As a result, a Drude peak appears for linear conductance [see Fig. 4(a)]. At the same time, the behavior of the optical nonlinearity enhancement resembles that of random composites due to the fact that the local field is spatially uniform for light polarized parallel to the plane of layers. On the other hand, in this case, the optical nonlinearity enhancement results only from the local field effect due to the random mixing of metal and dielectric components, while it results from not only the local field effect from above, but also from the compositional gradations for

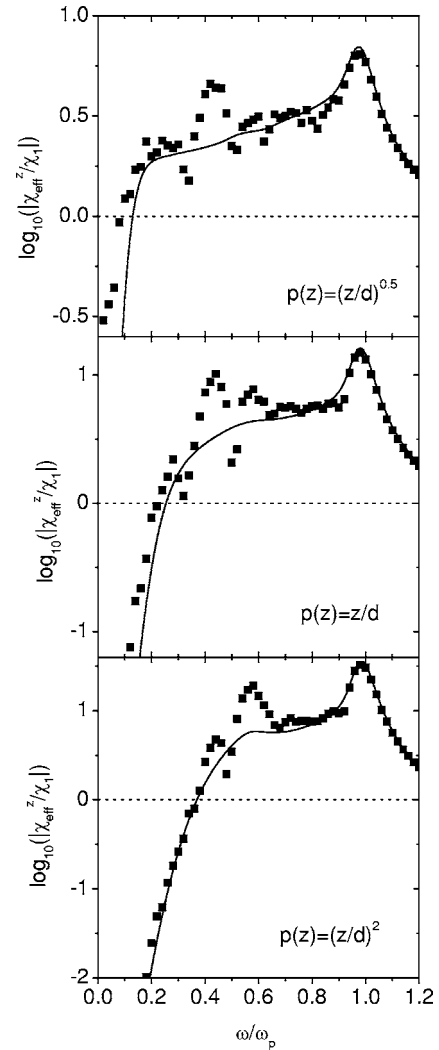


FIG. 6. Same as Fig. 2, but for power-law grade profile $p(z) = az^m$ with $a=1$ and different m .

electric field polarized perpendicular to the planes of the graded films. Therefore, large nonlinearity enhancement occurs for light polarized perpendicular to the planes of the graded films.

In the end, we take one step forward to investigate the optical nonlinearity enhancement in compositionally graded films with a power-law profile $p(z)=a(z/d)^m$ for different a with $m=1$ (Fig. 5) and different m with $a=1$ (Fig. 6). In Fig. 5, with increasing a , the total volume fraction increases, which causes the surface plasmon resonant band to be broadened over a range of frequencies. In addition, a sharp peak occurs at high frequency around the plasma frequency ω_p , and it exhibits blue-shift with increasing a . Again, we predict two prominent surface plasmon resonant peaks in the frequency region $0.4\omega_p < \omega < 0.6\omega_p$ and the locations of these peaks are almost independent of a . These properties cannot be observed in our theory. However, we still find that the effective medium approximation can be used to estimate the effective nonlinear optical susceptibility qualitatively. From Fig. 6, we note that as m increases, the magnitude of optical nonlinearity enhancement become strong, accompanied with

the narrow resonant band. Actually, with increasing m , more and more isolated metallic clusters appear in small z -slices. As a result, the surface plasmon resonance is enhanced and the optical nonlinearity is enlarged. Again, there are some discrepancies between the numerical simulation data and theoretical data, but our theoretical results capture the qualitative feature of the simulation data correctly.

V. CONCLUSION AND DISCUSSION

In this paper, we have studied both theoretically and numerically the effective linear and nonlinear optical properties in compositionally graded films, in which the volume fraction of metal component varies along the direction perpendicular to the film. On the theoretical side, we first adopt the effective medium approximation in conjunction with the spectral representation theory to obtain the local (equivalent) linear dielectric constant and third-order nonlinear susceptibility at z -slices. Then, we regard the compositionally graded film as a multilayer one to derive the effective linear and nonlinear optical properties. In order to check the validity of our theory, we perform numerical simulations on random resistor-capacitor networks, by taking into account the compositionally graded profile. Both our theory and numerical simulations show that the presence of compositional gradation is helpful to achieve large enhancement of optical nonlinear susceptibilities especially when the applied field is polarized perpendicular to the plane of layers. The theoretical results for linear response are in good agreement with numerical simulation data. Moreover, the theoretical results for nonlinear optical susceptibility are also in reasonable agreement with numerical simulation results. To one's interest, with numerical simulations, two surface plasmon resonant

peaks are found in the frequency region $0.4\omega_p \leq \omega \leq 0.6\omega_p$, which are totally neglected in our theory.

Here we would like to add a few comments. As we have invoked the Bruggeman effective medium approximation with spectral representation to study the equivalent (local) linear dielectric constant and third-order nonlinear susceptibility, our established formulas can be indeed valid for large volume fractions of metal component. In this connection, we predict the wide surface plasmon resonant bands. However, for small total volume fractions $p = \int_0^d dz p(z)$, the microstructure in each slice should be described by the one that metal particles are randomly embedded in the dielectric host. Then, one should expect sharp enhancement peaks in the optical nonlinearity instead of resonant bands.

Our present work can be extended in a variety of ways. For instance, both our theory and numerical simulations are limited to the weakly nonlinear case. That is to say, the contribution from the nonlinear response is much less than the one from the linear response. When the nonlinear response becomes strong, optical bistability may arise.^{31,32} It is of great interest to investigate the optical bistable properties in compositionally graded films. In addition, our calculations can be further generalized to the study of second and third harmonic generations in compositionally graded films. In this connection, numerical simulations are now being carried out to check our predictions in Ref. 33.

ACKNOWLEDGMENTS

This work was supported by the National Natural Science Foundation of China under Grant No. 10204017 (L.G.) and the Natural Science of Jiangsu Province under Grant No. BK2002038 (L.G.), and by Research Grants Council of Hong Kong SAR Government (K.W.Y.).

*Corresponding author. Email address: lgaophys@pub.sz.jsinfo.net

- ¹D. J. Bergman and D. Stroud, *Solid State Phys.* **46**, 147 (1992).
- ²A. K. Sarychev and V. M. Shalaev, *Phys. Rep.* **335**, 275 (2000), and references therein.
- ³V. M. Shalaev, *Nonlinear Optics of Random Media: Fractal Composites and Metal-Dielectric Film* (Springer-Verlag, Berlin, 2000).
- ⁴D. Cotter, R. J. Manning, K. J. Blow, A. D. Ellis, A. E. Kelly, D. Nasset, I. D. Phillips, A. J. Poustie, and D. C. Rogers, *Science* **286**, 1523 (1999).
- ⁵M. Yamanouchi, M. Koizumi, T. Hirai, and I. Shioda, in *Proceedings of the First International Symposium on Functionally Graded Materials*, Sendi, Japan, 1990.
- ⁶A. M. Freyria, E. Chignier, J. Guidollet, and P. Louisot, *Biomaterials* **12**, 111 (1991).
- ⁷H. Karacali, S. M. Risser, and K. F. Ferris, *Phys. Rev. E* **56**, 4286 (1997).
- ⁸D. A. Hughes and N. Hansen, *Phys. Rev. Lett.* **87**, 135503 (2001).
- ⁹D. S. Lin, J. L. Wu, S. Y. Pan, and T. C. Chiang, *Phys. Rev. Lett.* **90**, 046102 (2003).
- ¹⁰L. Gao, J. P. Huang, and K. W. Yu, *Phys. Rev. B* **69**, 075105

(2004).

- ¹¹J. P. Huang and K. W. Yu, *Appl. Phys. Lett.* **85**, 94 (2004).
- ¹²J. P. Huang and K. W. Yu, *Opt. Lett.* **30**, 275 (2005).
- ¹³S. Suresh and A. Mortensen, *Fundamentals of Functionally Graded Materials* (IOM Communications, London, 1998).
- ¹⁴Y. Miyamoto, W. A. Kaysser, B. H. Rabin, A. Kawasaki, and R. G. Ford, *Functionally Graded Materials: Design Processing and Applications* (Kluwer Academic, Dordrecht, 1999).
- ¹⁵H. M. Yin, G. H. Paulino, W. G. Buttler, and L. Z. Sun, *J. Appl. Phys.* **98**, 063704 (2005).
- ¹⁶P. M. Hui, X. Zhang, A. J. Markworth, and D. Stroud, *J. Mater. Sci.* **34**, 5497 (1999).
- ¹⁷J. P. Huang, L. Dong, and K. W. Yu, *Europhys. Lett.* **67**, 854 (2004).
- ¹⁸D. A. G. Bruggeman, *Ann. Phys.* **24**, 636 (1935).
- ¹⁹H. R. Ma, R. F. Xiao, and P. Sheng, *J. Opt. Soc. Am. B* **15**, 1022 (1998).
- ²⁰X. Zhang and D. Stroud, *Phys. Rev. B* **49**, 944 (1994).
- ²¹M. F. Law, Y. Gu, and K. W. Yu, *J. Phys.: Condens. Matter* **10**, 9549 (1998).
- ²²M. F. Law, Y. Gu, and K. W. Yu, *Phys. Rev. B* **58**, 12536 (1998).
- ²³X. Zhang and D. Stroud, *Phys. Rev. B* **52**, 2131 (1995).

- ²⁴P. M. Hui, C. Xu, and D. Stroud, *Phys. Rev. B* **69**, 014202 (2004).
- ²⁵D. Stroud and P. M. Hui, *Phys. Rev. B* **37**, 8719 (1988).
- ²⁶K. W. Yu, P. M. Hui, and D. Stroud, *Phys. Rev. B* **47**, 14150 (1993).
- ²⁷D. Stroud and V. E. Wood, *J. Opt. Soc. Am. B* **6**, 778 (1989).
- ²⁸L. Gao, K. W. Yu, Z. Y. Li, and Bambi Hu, *Phys. Rev. E* **64**, 036615 (2001).
- ²⁹G. L. Fischer, R. W. Boyd, R. J. Gehr, S. A. Jenekhe, J. A. Osaheni, J. E. Sipe, and L. A. Weller-Brophy, *Phys. Rev. Lett.* **74**, 1871 (1995).
- ³⁰O. Levy and D. J. Bergman, *Phys. Rev. B* **50**, 3652 (1994).
- ³¹K. P. Yuen and K. W. Yu, *J. Opt. Soc. Am. B* **14**, 1387 (1997).
- ³²L. Gao, L. Gu, and Z. Y. Li, *Phys. Rev. E* **68**, 066601 (2003).
- ³³L. Gao, *Phys. Rev. E* **71**, 067601 (2005).